

Numerical modeling of quasitransient backward Raman amplification of laser pulses in moderately undercritical plasmas with multicharged ions

A. A. Balakin,¹ N. J. Fisch,^{2,3} G. M. Fraiman,¹ V. M. Malkin,³ and Z. Toroker²

¹*Institute of Applied Physics RAS, Nizhnii Novgorod 603950, Russia*

²*Princeton Plasma Physics Laboratory, Princeton, New Jersey 08543, USA*

³*Department of Astrophysical Sciences, Princeton University, Princeton, New Jersey 08540, USA*

(Received 27 July 2011; accepted 20 September 2011; published online 20 October 2011)

It was proposed recently that powerful optical laser pulses could be efficiently compressed through backward Raman amplification in ionized low density solids, in spite of strong damping of the resonant Langmuir wave. It was argued that, even for nonsaturated Landau damping of the Langmuir wave, the energy transfer from the pump laser pulse to the amplified seed laser pulse can nevertheless be highly efficient. This work numerically examines such regimes of strong damping, called quasitransient regimes, within the simplest model that takes into account the major effects. The simulations indicate that compression of powerful optical laser pulses in ionized low density solids indeed can be highly efficient. © 2011 American Institute of Physics. [doi:10.1063/1.3650074]

I. INTRODUCTION

The technique of resonant backward Raman amplification (BRA) of laser pulses in plasmas¹ may make feasible exawatt and zetawatt optical laser pulses in reasonably compact devices.^{2–4} Key features of the BRA technique were verified experimentally in small aperture devices.^{5–9} Much larger aperture and higher power experiments are contemplated now. In particular, there is a possibility of backward Raman amplification of powerful laser pulses mediated by low density solids.¹⁰ Crude analytical estimates indicate that such BRA can be highly efficient, in spite of strong damping of the resonant Langmuir wave (which mediates energy transfer from a pump laser pulse to the amplified seed laser pulse). Numerical examination of these interesting BRA regimes within the simplest model is presented below. The model includes the following effects:

- The resonant Raman backscattering of the pump laser pulse into the counterpropagating short amplified seed laser pulse.
- Collisional and Landau damping of the resonant Langmuir wave (which mediates energy transfer from the pump laser pulse to the amplified seed laser pulse).
- The inverse bremsstrahlung of the pump and seed laser pulses.
- Plasma heating through the inverse bremsstrahlung of the pump and seed laser pulses and through the collisional and Landau damping of Langmuir wave.
- Relativistic electron nonlinearity of the amplified pulse, which imposes an upper limit on the allowed amplification length.
- Dispersion of the group velocity of the amplified pulses, which imposes a lower limit on the allowed duration of the input seed pulse.

In treating these effects, the current work employs the basic equations of the backward Raman amplification,

including terms describing the last two effects, the relativistic electron nonlinearity and group velocity dispersion,¹¹ and including the above-mentioned collisional effects that characterize the quasitransient regime.¹⁰ In particular, the Landau damping of the Langmuir wave mediating the resonant energy transfer is modeled here by the formula for the linear Landau damping in Maxwellian plasmas. As explained previously,¹⁰ this is not to imply that the actual Landau damping is not saturated but to verify that the BRA indeed can be efficient even for non-saturated linear Landau damping. In addition to the factors analyzed in Ref. 10, the current work crudely takes into account, in the manner similar to Refs. 12 and 13, the effect of strong fields on the collisional damping and inverse bremsstrahlung.

The model employed is 1-D but it captures the major effects. The amplification length, in practice, is limited by the relativistic electron nonlinearity of the amplified pulse. This cubic nonlinearity tends to cause filamentation of the pulse both in the longitudinal and transverse directions. To avoid the degradation of the pulse, the plasma length is taken short enough that the pulse is amplified and compressed only prior to the onset of these instabilities.¹ The forward Raman instability could also have been included within the 1D framework of equations that we consider. However, this instability can similarly be avoided by taking the plasma short enough, or by other means of suppression, such as through detuning.² The 1D equations that we employ thus describe well the plasma prior to the onset of these instabilities. It should be noted that, although the starting equations also describe compression of shorter wavelength pulses, like in the x-ray regime, we confine our specific illustrative examples to the optical regime.

Thus, this simple model captures the key features of the quasitransient backward Raman amplification (QBRA) regimes and can be used to verify when these regimes can be efficient. This may be particularly useful for modeling BRA of powerful optical pulses in ionized low-density solids, or

for BRA of intense x-ray pulses in denser plasmas, such as at solid densities.^{14,15} While many of the BRA features were described computationally in previous studies (see for instance, Refs. 16–28), it is only here that a simple computational model is employed to study the major physical processes that are associated specifically with the QBRA regime.

The paper is organized as follows: Sec. II introduces the basic QBRA equations employed here, Sec. III describes simulations of the QBRA in a regime of particular practical interest, and Sec. IV summarizes the results.

II. BASIC EQUATIONS

Equations for BRA, taking into account the above listed effects, can be presented in the form

$$\begin{aligned} a_t + c_a a_z &= V_3 f b - \nu_a a, & f_t &= -V_3 a b^* - \nu_f f, \\ b_t - c_b b_z &= -V_3 a f^* - i c'_b b_{tt} / 2c_b + i R |b|^2 b - \nu_b b. \end{aligned} \quad (1)$$

Here a , b , and f are envelopes of the long pump pulse, counterpropagating short pumped pulse (or seed pulse), and the resonant Langmuir wave, respectively; subscripts t and z signify time and space derivatives; c_a and c_b are group velocities of the pump and pumped pulses; c'_b is the derivative of the pumped pulse group velocity over the frequency; V_3 is the 3-wave coupling constant (real for appropriately defined wave envelopes), R is the coefficient of nonlinear frequency shift due to the relativistic electron nonlinearity; ν_a and ν_b are rates of the inverse bremsstrahlung for the pump and seed laser pulses, respectively; ν_f is the Langmuir wave damping. The dispersion and self-nonlinearity are taken into account only for the pumped pulse which is shorter and grows to intensities greater than that of the pump.

The group velocities c_a and c_b are expressed in the terms of the respective laser frequencies ω_a and ω_b as follows:

$$c_a = c \sqrt{1 - \frac{\omega_e^2}{\omega_a^2}}, \quad c_b = c \sqrt{1 - \frac{\omega_e^2}{\omega_b^2}}, \quad (2)$$

where c is the speed of light in vacuum,

$$\omega_e = \sqrt{\frac{4\pi n_e e^2}{m_e}} \quad (3)$$

is the electron plasma frequency, n_e is the electron plasma concentration, m_e is the electron mass, and e is the electron charge. Note that

$$\frac{c'_b}{c_b} = \frac{\omega_e^2}{\omega_b(\omega_b^2 - \omega_e^2)}, \quad (4)$$

which exhibits the group velocity dispersion of the seed pulse that becomes important at higher plasma density. The dominance at high density of this linear dispersion effect enables the neglect of nonlinear dispersion effects even when the seed pulse is only several optical cycles long.²⁹

The pump pulse envelope, a , will further be normalized such that the average square of the electron quiver velocity in the pump laser field, measured in units c^2 , will be $|a|^2$

$$\overline{v_{ea}^2} = c^2 |a|^2. \quad (5)$$

Then, the average square of the electron quiver velocity in the seed laser field and in the Langmuir wave field will be given by the formulas

$$\overline{v_{eb}^2} = c^2 |b|^2 \frac{\omega_a}{\omega_b}, \quad \overline{v_{ef}^2} = c^2 |f|^2 \frac{\omega_a}{\omega_f}. \quad (6)$$

The respective value of the 3-wave coupling constant is³⁰

$$V_3 = \frac{k_f c}{2} \sqrt{\frac{\omega_e}{2\omega_b}}, \quad (7)$$

where k_f is the wave number of the resonant Langmuir wave

$$k_f = k_a + k_b, \quad k_a c = \sqrt{\omega_a^2 - \omega_e^2}, \quad k_b c = \sqrt{\omega_b^2 - \omega_e^2}. \quad (8)$$

The frequency resonance condition is

$$\omega_b + \omega_f = \omega_a, \quad (9)$$

where ω_f is the Langmuir wave frequency. For Maxwellian plasma of electron temperature T_e ,

$$\omega_f = \omega_e \left(1 + \frac{3}{2} q_T\right), \quad (10)$$

assuming

$$q_T = \frac{k_f^2 T_e}{\omega_e^2 m_e} = \frac{T_e}{T_m} \ll 1. \quad (11)$$

The satisfaction of this inequality suggests that the frequency of the plasma wave may be approximated as just the plasma frequency; small deviations from the plasma frequency would be masked by other detuning effects such as pump chirping and plasma density gradients.

The nonlinear frequency shift coefficient R , corresponding to the above normalization of wave envelopes, is^{31–33}

$$R = \frac{\omega_e^2 \omega_a}{4\omega_b^2}. \quad (12)$$

The inverse bremsstrahlung rates ν_a and ν_b are expressed in the terms of the electron-ion collision rate ν_{ei} by formulas³⁴

$$\nu_a = \nu_{ei} \frac{\omega_e^2}{2\omega_a^2}, \quad \nu_b = \nu_{ei} \frac{\omega_e^2}{2\omega_b^2}. \quad (13)$$

The Langmuir wave damping consists of the collisional and Landau damping

$$\nu_f = \nu_{ei}/2 + \nu_{Lnd}. \quad (14)$$

The Landau damping is crudely modeled by the linear Landau in Maxwellian plasma³⁵

$$\nu_{Lnd} = \frac{\omega_e \sqrt{\pi}}{(2q_T)^{3/2}} \exp\left(-\frac{1}{2q_T} - \frac{3}{2}\right). \quad (15)$$

Formula (15) is quantitatively justified under conditions when Maxwellization has time enough to occur for the resonant electrons responsible for the Landau damping. Otherwise, this formula overestimates the Landau damping because of flattening the resonant electron distribution. In transient BRA regimes, where collisions have not enough time to occur within the amplified pulse duration even for the thermal electrons, the faster resonant electron apparently are not Maxwellian. The model can be used nevertheless to verify that highly efficient BRA can be sustained even for the overestimated Landau damping.

The field-affected rate of electron-ion collisions is crudely modeled by the formula^{12,13}

$$\nu_{ei} = \frac{2}{3} \sqrt{\frac{2\pi}{m_e}} \frac{Z\Lambda n_e e^4}{T_e^{1/2}(T_e + T_{enl})}, \quad (16)$$

where Λ is the Coulomb logarithm, Z is the plasma ion charge, and

$$T_{enl} = m_e c^2 \left(|a|^2 + |b|^2 \frac{\omega_a}{\omega_b} + |f|^2 \frac{\omega_a}{\omega_f} \right). \quad (17)$$

The electron plasma heating is modeled by equation

$$\frac{\partial T_e}{\partial t} = \frac{2}{3} \left(\nu_{ei} T_{enl} + 2m_e c^2 \nu_{Lnd} |f|^2 \frac{\omega_a}{\omega_f} \right). \quad (18)$$

III. NUMERICAL RESULTS

Consider BRA in a uniform plasma layer of width L . The duration of pump interacting with seed within such a layer is $L_{pmp} = L(1 + c_a/c_b)$. For the pump of constant amplitude a_0 , it is convenient to measure wave amplitudes in units of a_0 . This means the following redefining of wave amplitudes:

$$a \rightarrow a_0 a, \quad b \rightarrow a_0 b, \quad f \rightarrow a_0 f. \quad (19)$$

By measuring the time t in units $1/V_3 a_0$, distance z in units $c_a/V_3 a_0$, damping rates ν_a, ν_b , and ν_f in units $V_3 a_0$, nonlinear frequency shift coefficient R in units V_3/a_0 , the basic equations (1) can be rewritten in the form

$$a_t + a_z = fb - \nu_a a, \quad f_t = -ab^* - \nu_f f, \quad (20)$$

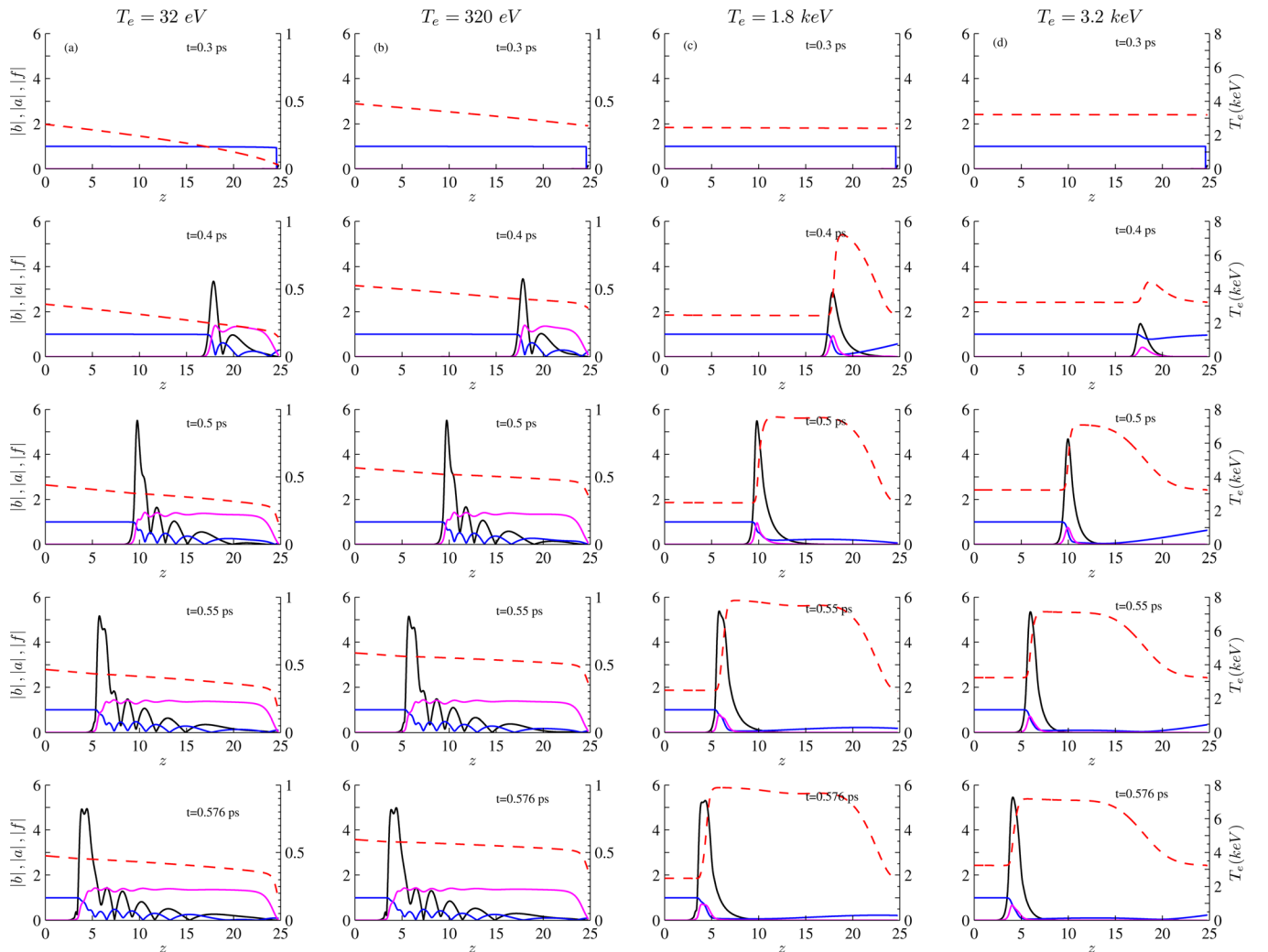


FIG. 1. (Color online) Dynamics of BRA in plasma with ion charge $Z=6$ for several initial plasma temperatures: 32 eV (a), 320 eV (b), 1.8 keV (c), and 3.2 keV (d). Black solid line shows the seed pulse amplitude, gray (blue online) solid curve is the pump pulse amplitude, light gray (magenta online) solid line is the Langmuir wave amplitude, and red dashed curve is the temperature profile.

$$b_t - b_z c_b / c_a = -a f^{*} - \kappa b_{tt} + i R |b|^2 b - \nu_b b, \quad (21)$$

$$\kappa = c_b' / 2 c_b V_3 a_0$$

(and complemented by the, respectively, transformed Equation (18)).

Let the pump wavelength be $\lambda = 0.351 \mu\text{m}$, like for NIF laser pulses.³⁶ Let the ratio of the plasma frequency to the pump laser frequency be 0.3, $q_L = \omega_e / \omega_a = 0.3$, corresponding to the electron plasma density $n_e = 8.2 \cdot 10^{20} \text{ cm}^{-3}$, like that for the lowest density solids. Let the width of the plasma be $L = 25$ linear Raman lengths, $25 c_a / V_3 a_0$. This is $87.5 \mu\text{m}$ for $a_0 = 6 \cdot 10^{-10} \lambda [\mu\text{m}] \sqrt{I_a [\text{W}/\text{cm}^2]} = 00411$, corresponding to the pump intensity of $38 \text{ PW}/\text{cm}^2$ (which is below the wave-breaking threshold equal to $61 \text{ PW}/\text{cm}^2$). The respective length of the pump pulse is $25(1 + c_a / c_b) = 51.41 = \Delta_a$ linear Raman lengths. The initial seed pulse is taken to be Gaussian with the maximum intensity of $2.5 \text{ PW}/\text{cm}^2$ and full width at half maximum (FWHM) of $2\pi / \omega_e = 3.89 \text{ fs}$. This corresponds to the initial integrated amplitude $\epsilon = \int b dt = 0.15$. The Coulomb logarithm in Eq. (16) is taken to be $\Lambda = 3.14$. For these initial conditions, one obtains $T_m = 18.72 \text{ keV}$. Hence, for temperatures below about 1 keV , the detuning of the plasma wave frequency can be neglected. For higher initial temperatures, the detuning might be important, but the temperature grows less since the heating is smaller (because of the lower electron-ion collision rate). This means that the detuning is approximately constant and can be compensated by chirping either the pump or seed pulses or by introducing gradients in the plasma density.

Figure 1 shows evolution of the seed, pump and Langmuir wave amplitudes, and plasma temperature in plasma

with ion charge $Z = 6$ for several initial plasma temperatures 32 eV (1a), 320 eV (1b), 1.8 keV (1c), and 3.2 keV (1d).

At smaller initial plasma temperatures, shown in Figs. 1(a) and 1(b), the Langmuir wave damping appears to be negligible. This is because the Landau damping is inherently small in this region, while the collisional damping is reduced due to the high quiver velocity of electrons in strong electromagnetic field. As a result, BRA resembles that in the transient regime.^{1,37} The beginning of the leading spike splitting seen at the final BRA stages indicates that the amplification length cannot be increased, because of self-phase modulation instability associated with the relativistic electron nonlinearity.

At larger initial plasma temperatures, shown in Figs. 1(c) and 1(d), the Langmuir wave appears to be noticeably damped even within the leading amplified spike duration due to the strong Landau damping. Therefore, the BRA occurs in quasitransient regimes.^{10,38} In these regimes, the secondary spikes are suppressed, and the plasma is clearly heated within the amplified spike duration, which makes the Landau damping even stronger. It can extend the linear BRA stage and delay the pump depletion as seen from Fig. 1(d).

Figure 2(a) shows the maximal output pulse intensity

$$G = \frac{\omega_b}{\omega_a} \max_t |b(z=0, t)|^2, \quad (22)$$

and Fig. 2(b) shows the fraction of the pumped energy containing in the output pulse,

$$\eta = \frac{\omega_b}{\omega_a} \frac{\int_{-\infty}^{\infty} |b(z=0, t)|^2 dt}{\Delta_a}, \quad (23)$$

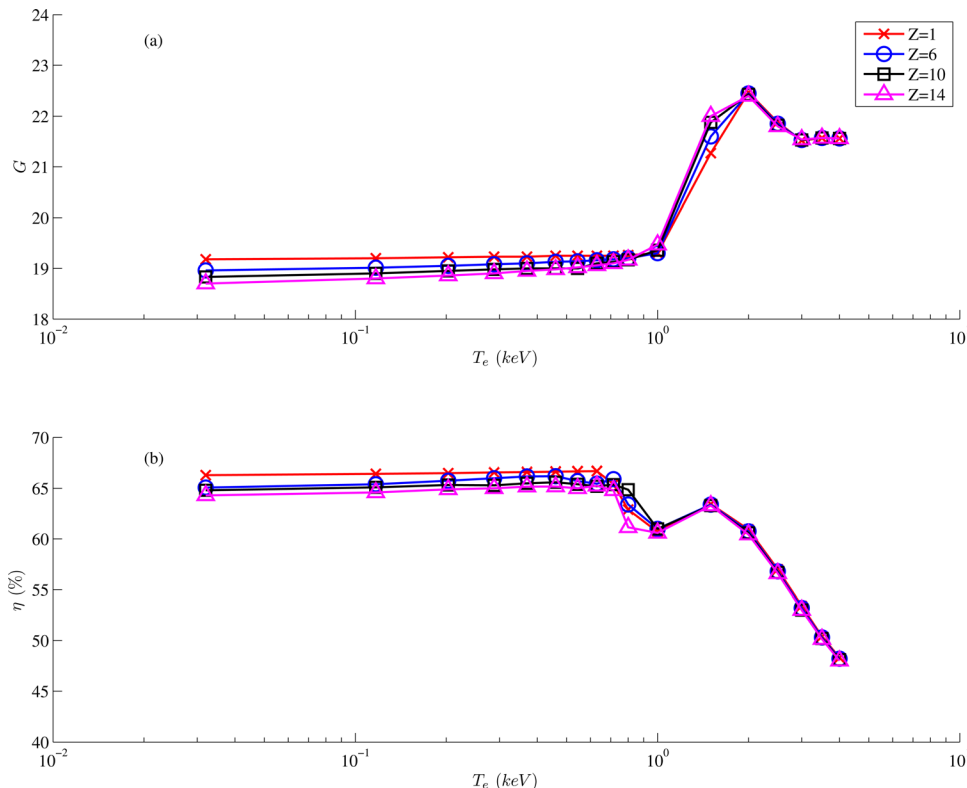


FIG. 2. (Color online) Maximal output pulse intensity G (a) and BRA efficiency η (b) as functions of the initial plasma temperature for plasma ion charges $Z=1$ (red cross solid line), $Z=6$ (blue circle solid line), $Z=10$ (black square solid line), and $Z=14$ (magenta triangle solid line).

as functions of the initial plasma electron temperature for several different plasma ion charges: $Z = 14$ (silicon, Si), $Z_{\text{eff}} = 10$ (silica, SiO₂), $Z = 6$ (carbon, C), and $Z = 1$ (hydrogen, H).

As seen, the results are nearly the same for all these values of Z . The results also appear to be not sensitive ($\eta \approx 65\%$ and $G \approx 19$) to the initial plasma temperature up to about 1 keV. At initial temperatures exceeding 1 keV, the Langmuir wave Landau damping becomes important. Some increase of the maximal output pulse intensity in this regime (Fig. 2(a)) is associated with the Langmuir wave suppression which prevents energy flowing back from the leading spike to the pump. This effect also causes a decrease of the efficiency η (Fig. 2(b)) due to the suppression of the secondary spikes and trailing part of the leading spike.

Figure 3 shows how BRA dynamics is affected by the Langmuir damping ν_f within even a simpler model where relativistic electron nonlinearity and dispersion effects are absent. Fig. 3(a) shows the classical π -pulse regime corre-

sponding to $\nu_f = 0$. For the Langmuir damping 3 times larger than the linear Raman growth rate (Fig. 3(b)), the amplified pulse has already just a single spike. For the Langmuir damping 10 times larger than the linear Raman growth rate (Fig. 3(c)), the pump depletion is delayed so much that longer plasma length (66.75 linear Raman lengths) is needed to obtain the same output pulse maximal intensity as in Fig. 3(b).

Fig. 4 shows BRA dynamics within the model neglecting the relativistic electron nonlinearity and dispersion effects, like Fig. 3, but using the above formulas for the Langmuir wave damping (rather than the constant damping used in Fig. 3). The plasma ion charged is taken to be $Z = 6$. At temperatures of 32 and 320 eV (Figs. 4(a) and 4(b)), the amplified pulse has a π -pulse profile, like in Fig. 3(a), because of the smallness of the Langmuir wave damping at such temperatures. For higher temperatures, $T_e = 1.8$ keV (Fig. 4(c)), and even more $T_e = 3.2$ keV (Fig. 4(d)), the Landau damping becomes important and suppresses secondary amplified spikes. The case of 10 times more intense initial

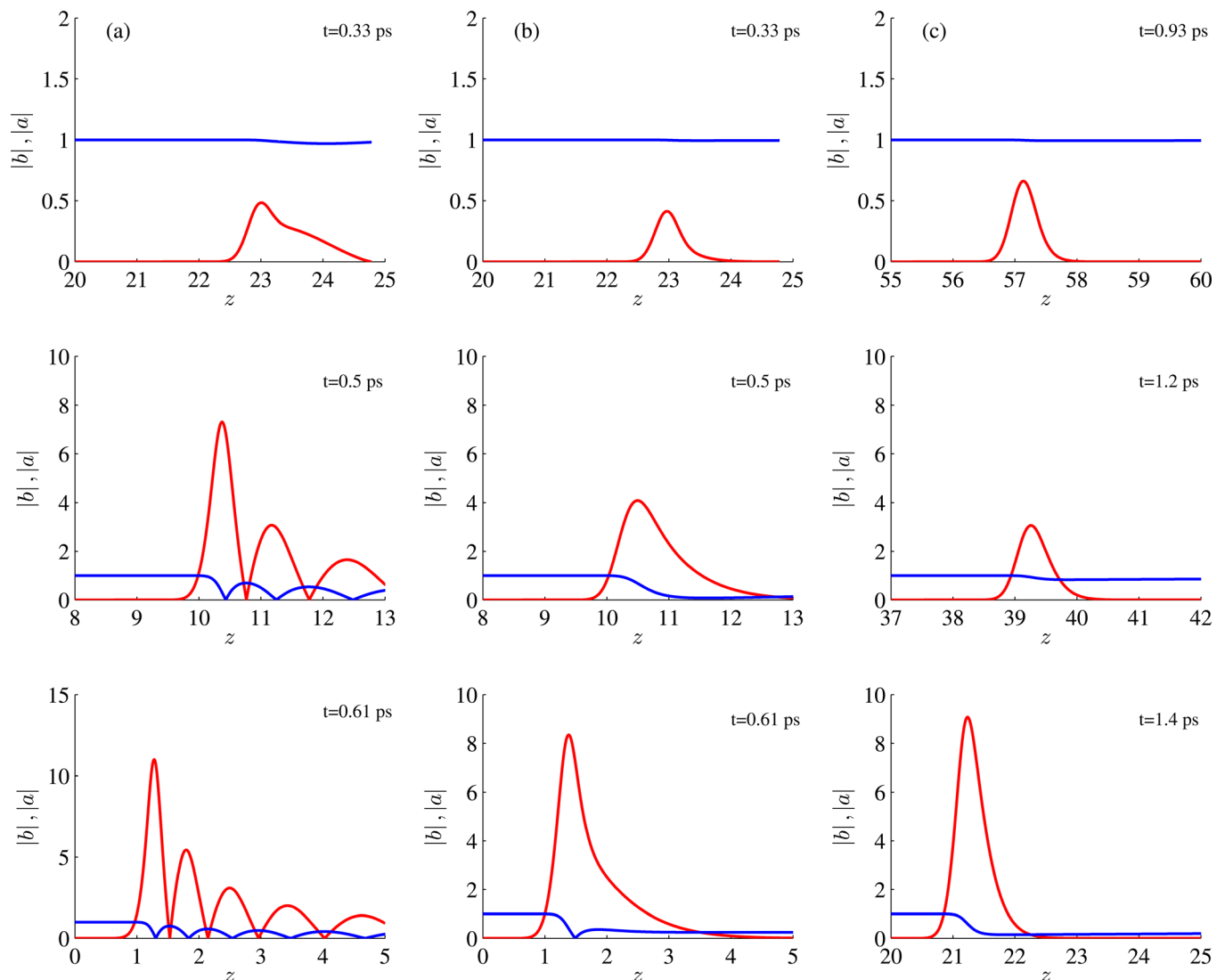


FIG. 3. (Color online) BRA dynamics neglecting the relativistic electron nonlinearity and dispersion effects, for the Langmuir damping to 0 (a), 3 (b), and 10 (c) linear Raman growth rates. The solid line depicting the traveling spike (red online) shows the seed pulse amplitude, the solid line with magnitude of 1 at the left boundary (blue online) is pump pulse amplitude. Note that a longer BRA length is used in case (c)

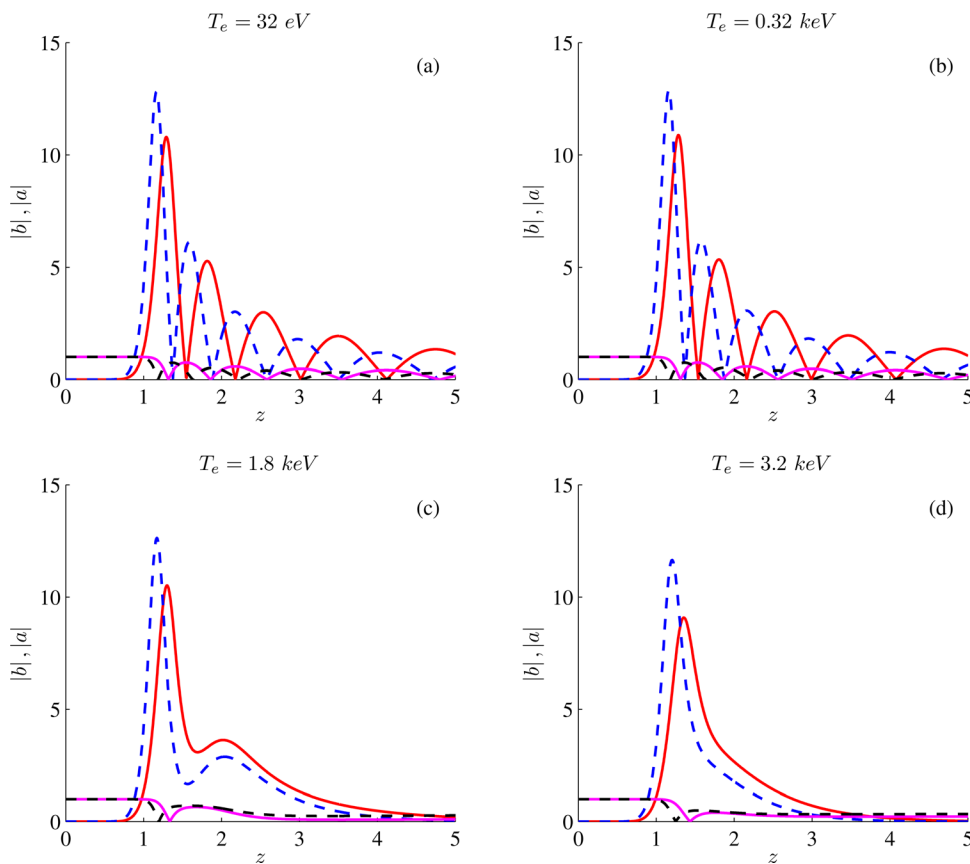


FIG. 4. (Color online) BRA dynamics neglecting the relativistic electron nonlinearity and dispersion effects, in plasmas with ion charge $Z=6$ and initial temperatures of 32 eV, 0.32, 1.8, and 3.2 keV. The solid line with magnitude of 1 at the left boundary (magenta online) is pump pulse amplitude, spike (red online) is the seed pulse amplitude. Dashed lines show the same for the 10 times more intense initial seed pulse.

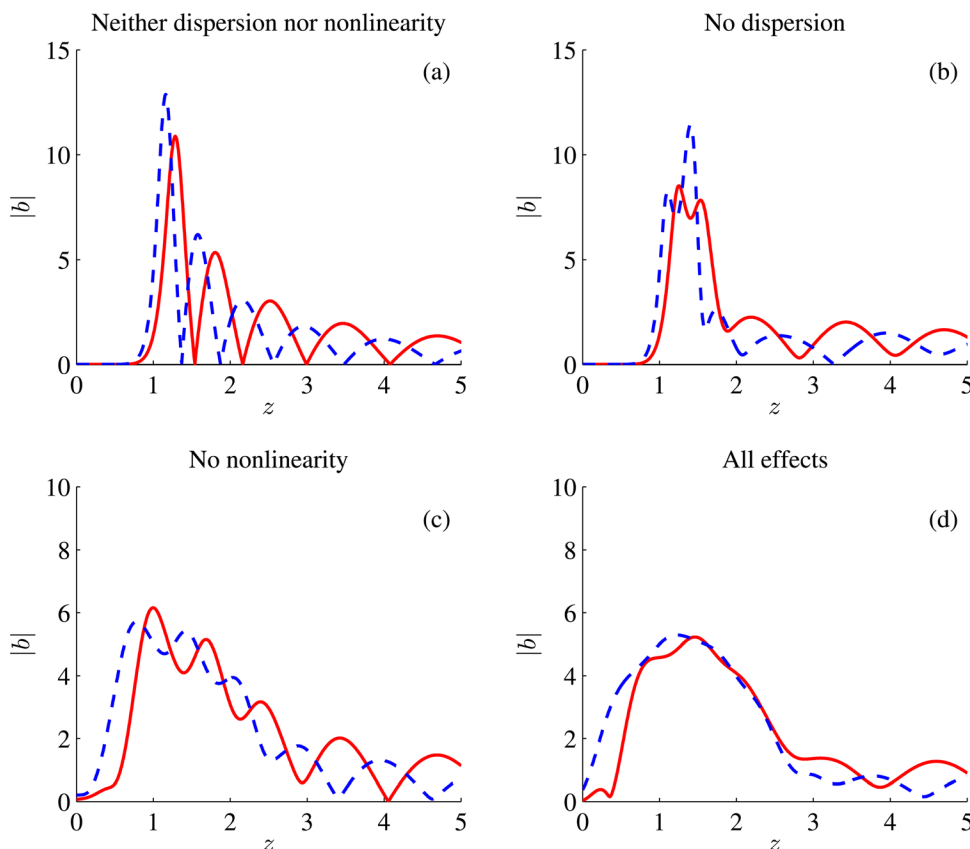


FIG. 5. (Color online) Effects of the relativistic electron nonlinearity and dispersion on BRA in plasma with ion charge $Z=6$ and initial electron plasma temperature 0.32 keV. Both the relativistic electron nonlinearity and dispersion turned off (a), the relativistic electron nonlinearity turned on and the dispersion turned off (b), the relativistic electron nonlinearity turned off and the dispersion turned on (c), and both the relativistic electron nonlinearity and dispersion turned on (d). Dashed lines show BRA for the 10 times more intense initial seed.

seed pulse (25 PW/cm^2) is also shown in Fig. 4 (dashed lines). As seen, the results are not very sensitive to the initial pulse intensity.

Figure 5 shows how the relativistic electron nonlinearity and dispersion affect BRA dynamics in plasma with the initial temperature 0.32 keV and ion charge $Z=6$. Figure 5(a) shows the amplified pulse evolution neglecting both the relativistic electron nonlinearity and dispersion effects. The effect of the relativistic electron nonlinearity (without dispersion) is shown in Fig. 5(b). The effect of the dispersion (without relativistic electron nonlinearity) is shown in Fig. 5(c). The joint effect of the relativistic electron nonlinearity and dispersion is shown in Fig. 5(d). The case of 10 times more intense initial seed pulse (25 PW/cm^2) is shown in Fig. 5 by dashed lines. As seen, the dispersion effect merges few leading amplified spikes into a single one. It is also seen that the results are not very sensitive to the initial seed intensity.

IV. CONCLUSION

Numerical modeling was performed describing QBRA in plasmas within the simplest model taking into account the major effects, such as, Raman backscattering, relativistic electron nonlinearity, dispersion of the laser group velocities, collisional and Landau damping of the resonant Langmuir wave, inverse bremsstrahlung of the pump, and seed laser pulses and plasma heating through these effects. In particular, the QBRA regime was explored for 351 nm light, like the NIF laser, in plasmas of electron concentration $n_e = 8.2 \cdot 10^{20} \text{ cm}^{-3}$, corresponding to the density in the range of the lowest density solids. The simulations show that QBRA in this important regime can indeed be efficient.

ACKNOWLEDGMENTS

This work was supported by RFBR Grant No. 11-02-01070-a, by DOE Contract DE-AC0209-CH11466, and by the NNSA under the SSAA Program through DOE Research Grant No. DE-FG52-08NA28553.

¹V. M. Malkin, G. Shvets, and N. J. Fisch, *Phys. Rev. Lett.* **82**, 4448 (1999).

²V. M. Malkin, G. Shvets, and N. J. Fisch, *Phys. Plasmas* **7**, 2232 (2000).

³N. J. Fisch and V. M. Malkin, *Phys. Plasmas* **10**, 2056 (2003).

⁴V. M. Malkin and N. J. Fisch, *Phys. Plasmas* **12**, 044507 (2005).

⁵Y. Ping, W. Cheng, S. Suckewer, D. S. Clark, and N. J. Fisch, *Phys. Rev. Lett.* **92**, 175007 (2004).

⁶W. Cheng, Y. Avitzour, Y. Ping, S. Suckewer, N. J. Fisch, M. S. Hur, and J. S. Wurtele, *Phys. Rev. Lett.* **94**, 045003 (2005).

⁷J. Ren, A. M. S. Li, S. Suckewer, N. A. Yampolsky, V. M. Malkin, and N. J. Fisch, *Phys. Plasmas* **15**, 056702 (2008).

⁸N. A. Yampolsky, N. J. Fisch, V. M. Malkin, E. J. Valeo, R. Lindberg, J. Wurtele, J. Ren, A. M. S. Li, and S. Suckewer, *Phys. Plasmas* **15**, 113104 (2008).

⁹N. A. Yampolsky and N. J. Fisch, *Phys. Plasmas* **18**, 056711 (2011).

¹⁰V. M. Malkin and N. J. Fisch, *Phys. Plasmas* **17**, 073109 (2010).

¹¹V. M. Malkin and N. J. Fisch, *Phys. Rev. Lett.* **99**, 205001 (2007).

¹²G. M. Fraiman, A. A. Balakin, and V. A. Mironov, *Phys. Plasmas* **8**, 2502 (2001).

¹³A. Brantov, W. Rozmus, R. Sydora, C. E. Capjack, V. Y. Bychenkov, and V. T. Tikhonchuk, *Phys. Plasmas* **10**, 3385 (2003).

¹⁴V. M. Malkin, N. J. Fisch, and J. S. Wurtele, *Phys. Rev. E* **75**, 026404 (2007).

¹⁵S. Son, S. Ku, and S. J. Moon, *Phys. Plasmas* **17**, 114506 (2010).

¹⁶A. A. Solodov, V. M. Malkin, and N. J. Fisch, *Phys. Plasmas* **10**, 2540 (2003).

¹⁷R. L. Berger, D. S. Clark, A. A. Solodov, E. J. Valeo, and N. J. Fisch, *Phys. Plasmas* **11**, 1931 (2004).

¹⁸G. M. Fraiman, N. A. Yampolsky, V. M. Malkin, and N. J. Fisch, *Phys. Plasmas* **9**, 3617 (2002).

¹⁹P. Mardahl, H. J. Lee, G. Penn, J. S. Wurtele, and N. J. Fisch, *Phys. Lett. A* **296**, 109 (2002).

²⁰D. S. Clark and N. J. Fisch, *Phys. Plasmas* **10**, 4837 (2003).

²¹A. A. Balakin, G. M. Fraiman, N. J. Fisch, and V. M. Malkin, *Phys. Plasmas* **10**, 4856 (2003).

²²D. S. Clark and N. J. Fisch, *Phys. Plasmas* **10**, 4848 (2003).

²³D. S. Clark and N. J. Fisch, *Laser Part. Beams* **23**, 101 (2005).

²⁴A. A. Balakin, G. M. Fraiman, N. J. Fisch, and S. Suckewer, *Phys. Rev. E* **72**, 036401 (2005).

²⁵M. S. Hur, I. Hwang, H. J. Jang, and H. Suk, *Phys. Plasmas* **13**, 073103 (2006).

²⁶D. S. Clark and N. J. Fisch, *Phys. Plasmas* **10**, 3363 (2003).

²⁷T.-L. Wang, D. S. Clark, D. J. Strozzi, S. C. Wilks, S. F. Martins, and R. K. Kirkwood, *Phys. Plasmas* **17**, 023109 (2010).

²⁸R. M. G. M. Trines, F. Fiuza, R. Bingham, R. A. Fonseca, L. O. Silva, R. A. Cairns, and P. A. Norreys, *Nat. Phys.* **7**, 87 (2010).

²⁹A. A. Balakin, A. G. Litvak, V. A. Mironov, and S. A. Skobelev, *Phys. Rev. A* **80**, 063807 (2009).

³⁰W. L. Kruer, *The Physics of Laser Plasma Interactions* (Addison-Wesley, Reading, MA, 1988), pp. 73–85.

³¹A. G. Litvak, *Zh. Eksp. Teor. Fiz.* **57**, 629 (1969) [*Sov. Phys. JETP* **30**, 344 (1970)].

³²C. Max, J. Arons, and A. B. Langdon, *Phys. Rev. Lett.* **33**, 209 (1974).

³³G.-Z. Sun, E. Ott, Y. C. Lee, and P. Guzdar, *Phys. Fluids* **30**, 526 (1987).

³⁴I. P. Shkarofsky, T. W. Johnston, and M. P. Bachynsky, *The Particle Kinetics of Plasmas* (Addison-Wesley, Reading, 1966), p. 258.

³⁵E. M. Lifshitz and L. P. Pitaevsky, *Fizicheskaya Kinetika* (Nauka, Moskva, 1979) p. 168.

³⁶See <http://www.llnl.gov/nif/project> for The National Ignition Facility Project website.

³⁷V. M. Malkin, G. Shvets, and N. J. Fisch, *Phys. Rev. Lett.* **84**, 1208 (2000).

³⁸V. M. Malkin and N. J. Fisch, *Phys. Rev. E* **80**, 046409 (2009).